Supporting information

Efficient Photocatalytic Conversion of Benzene to Phenol on Stabilized Subnanometer WO_3 Quantum Dots

Akihide Ohno[a] ,Hiroto Watanabe[a,b], Takahiro Matsui[a], Shoichi Somekawa[b], Mai Tomisaki[a], Yasuaki Einaga[a], Yuya Oaki[a], Hiroaki Imai[a]

[a] *School of Integrated Design Engineering, Faculty of Science and Technology, Keio University, 3-14-1 Hiyoshi, Kohoku-ku, Yokohama 223-8522, Japan.*

[b] *Tokyo Metropolitan Industrial Technology Research Institute, 2-4-10 Aomi. Koto-ku, Tokyo 135-0064, Japan.*

Experimental section

Synthesis of mesoporous silica

Trimethylstearyl ammonium chloride, tetraethyl orthosilicate, and HCl_{aq} (pH 2.0) were mixed at a molar ratio of 0.2 : 1.0 : 4.0. The mixture was stirred at 298 K, and the resultant gel was dried at 333 K for 24 h and calcined at 873 K for 3 h in air. Details of the experimental procedures have been described in previous works.[S1,S2] The resultant mesopore size was estimated to be 2.7 nm based on the adsorption isotherms of nitrogen using Micromeritics 3Flex-3MP (Fig. S1 in the Electronic Supporting Information (ESI)). The MPSs have a wormhole structure that is suitable for the preparation of QDs.

Synthesis of WO_3 QDs with mesoporous silica template

A precursor suspension was prepared by dissolving 2.0 g of tungstic acid (H_2WO_4) powder in a mixture of 20 cm^3 of H_2O and 20 cm^3 of a 17.5 % H_2O_2 aqueous solution. The suspension was stirred for 1 week to obtain a colorless transparent solution of peroxotungstic acid. We prepared WO_3 QDs by vacuum drying and subsequent calcination after impregnating MPSs with an aqueous solution of peroxotungstic acid. The impregnation volume of the solution was fixed to be equal to the pore volume of the silica matrix. The resultant powder was dried under reduced pressure and then calcined at 723 K for 3 h in air.

Synthesis of Pt-WO_3

The bulk WO_3 powder was dispersed in a mixture of 70 cm^3 of H_2O and 0.01 cm^3 of a 0.2M H_2PtCl_6 aqueous solution. The suspension was irradiated by UV light (270–410 nm) from an ultra-high-pressure mercury lamp through two cut-off filters for 2 h. Then 10 cm^3 of methanol was added to the reaction mixture and continuously irradiated for 2 h. The products were collected by filtration and washed with water. The sample was dried under air at 333 K for overnight to obtain Pt-WO_3.

Photochemical dissolution test

We performed preliminary photochemical dissolution of WO_3 QDs in water with and without benzene under UV illumination. The MPS powder containing WO_3 QDs was dispersed in water and stirred in the presence of air in a closed system. The contents were irradiated by UV light (270–410 nm) from an ultra-high-pressure mercury lamp through two cut-off filters.

Photochemical production of H_2O_2

We performed photocatalytic production of H_2O_2 in water under UV illumination. The MPS powder containing WO_3 QDs (the initial mass of WO_3: 10 mg) or 10 mg of bulk WO_3, 29 cm^3 of H_2O, and 1 cm^3 of acetic acid were mixed and then stirred in a closed system. The suspension was illuminated by UV light (270–410 nm) from an ultra-high-pressure mercury lamp (Ushio USH-250SC2) through two cut-off filters. The amount of H_2O_2 produced was determined by using following reaction.[S3]

$$H_2O_2 + 3I^- + 2H^+ \rightarrow I^{3-} + 2H_2O$$

The reaction mixture was mixed with aqueous solution of KI (0.4 M) and $C_8H_5KO_4$ (0.1 M) to produce I^{3-}. The amount of H_2O_2 produced was determined by measuring intensity of 350 nm absorption (absorption of I^{3-}) from UV-vis spectra.

Photochemical conversion of benzene to phenol

We evaluated the photocatalytic activity for the conversion of benzene to phenol. The MPS powder containing WO_3 QDs (the initial mass of WO_3: 10 mg), 29 cm^3 of H_2O, and 1 cm^3 of benzene were mixed and then stirred with air in a closed system. The suspension at pH 6 was illuminated by UV light (270–410 nm) from an ultra-high-pressure mercury lamp (Ushio USH-250SC2) through two cut-off filters. We used commercial TiO_2 (Evonik P25) and WO_3 (Kanto Chemical) powders as references. The amount of phenol produced was measured by high performance liquid chromatography (HPLC, Prominence).

Photochemical decomposition of phenol

Decomposition of phenol with photocatalysts was evaluated using a 30 cm^3 aqueous solution system containing 2.5 $mmol/dm^3$ phenol and 10 mg of catalysts. The amounts of CO_2 that were generated from the solution in a closed vessel were measured by gas chromatography (Aglilent 3000) under illumination of UV light (270–410 nm). We loaded Pt on commercial WO_3 powder (40 mg) in a 70 cm^3 aqueous solution containing 0.25 $\mu mol/dm^3$ H_2PtCl_6 and 10 cm^3 ethanol. The powder in the suspension was illuminated for 2 h under UV light from an ultra-high-pressure mercury lamp and then recovered through filtration, washing with purified water, and drying at 60°C.

Characterization

The size and structure of the WO_3 QDs were characterized using transmission electron microscopy (TEM, FEI Tecnai F20) and Raman scattering spectroscopy (Renishaw in Via with a 532 nm laser as an excitation light). The Raman signals of the WO_3 QDs were enhanced using the surface-enhanced Raman scattering (SERS) technique. Metallic Ag

particles were photodeposited on WO_3 QDs by injecting a $AgNO_3$ solution (0.1 mol/dm^3) into the pores of the silica matrix and subsequent UV irradiation (254 nm) using a UV lamp (AS ONE SLUV-6) for 8 h. The contents of WO_3 in the silica matrix were evaluated by the X-ray fluorescence (XRF, Shimazu EDX-8100) technique. The band structure of the WO_3 QDs was estimated from the absorption edge monitored by UV-vis absorption spectra (JASCO V-670). We prepared WO_3 QDs/phenol complexes to evaluate the CBM of WO_3 QDs experimentally. The derivatives of phenol on a metal oxide give photoinduced charge-transfer (CT) excitation from

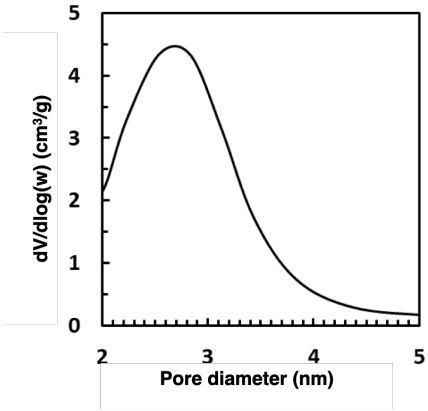

Fig. S1 The pore-size distribution of the MPS matrix using the Barrett-Joyner-Halenda (BJH) method according to nitrogen adsorption isotherms.

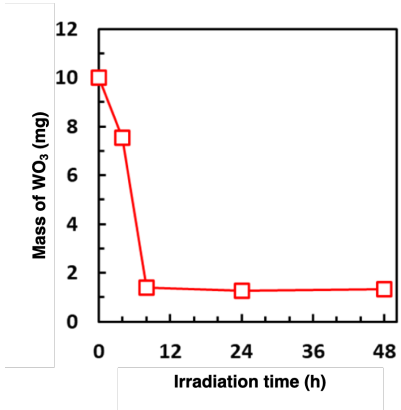

Fig. S2 The mass variation of WO_3 QDs in the MPS matrix estimated by XRF with photochemical dissolution for certain periods.

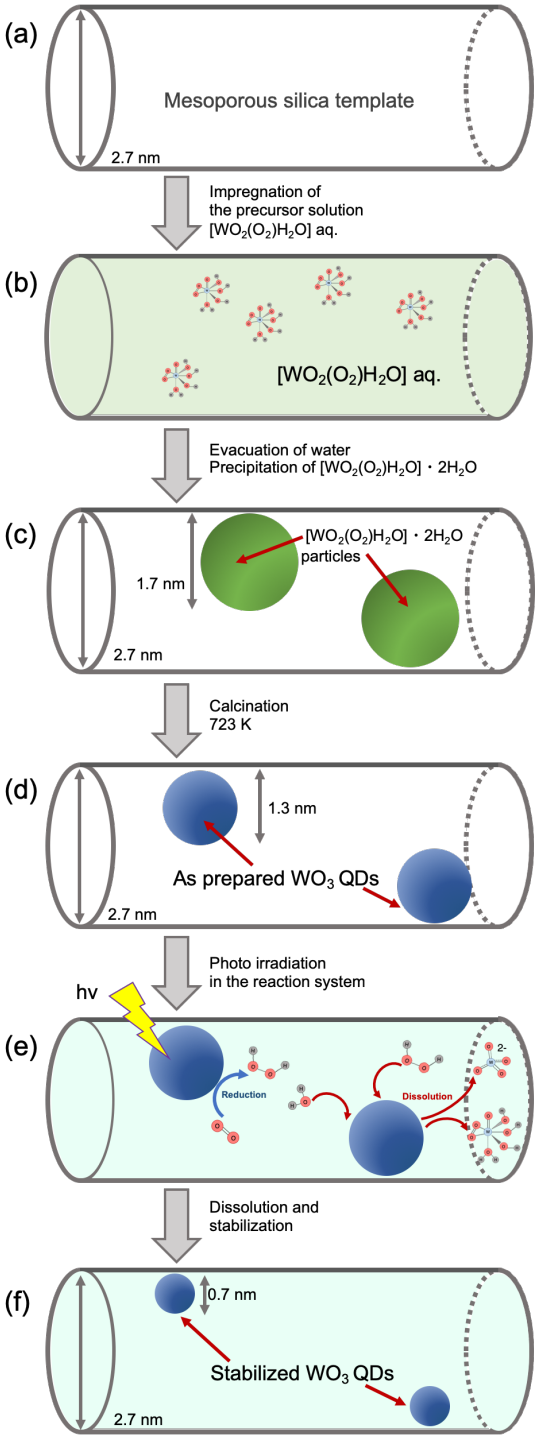

Fig. S3 Schematic illustration of the stabilized WO_3 QDs formation. (a) Mesoporous silica template. (b) Impregnation of the precursor solution. (c) Precipitation of the precursor. (d) Formation of as-prepared WO_3 QDs. (e) Photocatalytic dissolution of as-prepared WO_3 QDs. (f) Formation of stabilized WO_3 QDs.

Evaluation of the energy levels of the CBM and the VBM

For the determination of the band-edge energies of the QDs, we utilized a charge-transfer excitation between semiconductors and organic molecules. When the organic molecules, such as phenolic compounds, adsorbed on the semiconductor surface, a charge-transfer excitation from the HOMO level of the organic molecules to the conduction band of semiconductors takes place by a photon absorption. This complexation causes a distinct color change of the materials owing to the formation of charge-transfer band. In this study, we measured a charge-transfer excitation energy (E_{CT}) of WO_3-phenol complex from UV-Vis spectra to determine the CBM and VBM levels (Fig. S4). The WO_3-phenol complex was produced by contacting an excess amount of eutectic phenol with WO_3. We obtained the CBM and VBM levels of WO_3 QDs using the following equations.

$$E_{CBM} = E_{HOMO}\,(\text{phenol}) - E_{CT}$$

$$E_{VBM} = E_{CBM} + E_g$$

In this study, E_{HOMO} (phenol) was directly determined by using a photoemission yield spectroscopy in air (PYSA) (Fig. S5). E_g were determined from UV-Vis spectra (Fig. 2 in the main text).

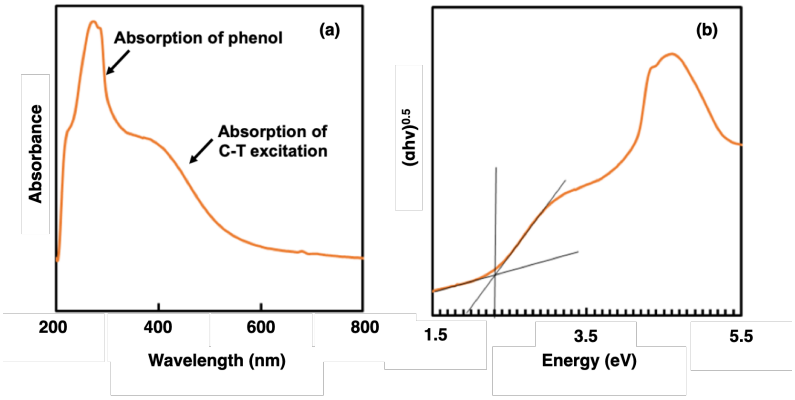

Fig. S4 A UV-vis absorption spectrum (a) and a Tauc plot (b) of the charge-transfer complex between the stabilized WO_3 QDs and phenol.

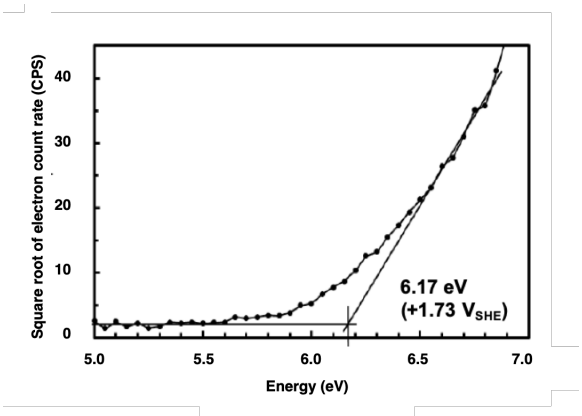

Fig. S5 A PYSA spectrum of phenol

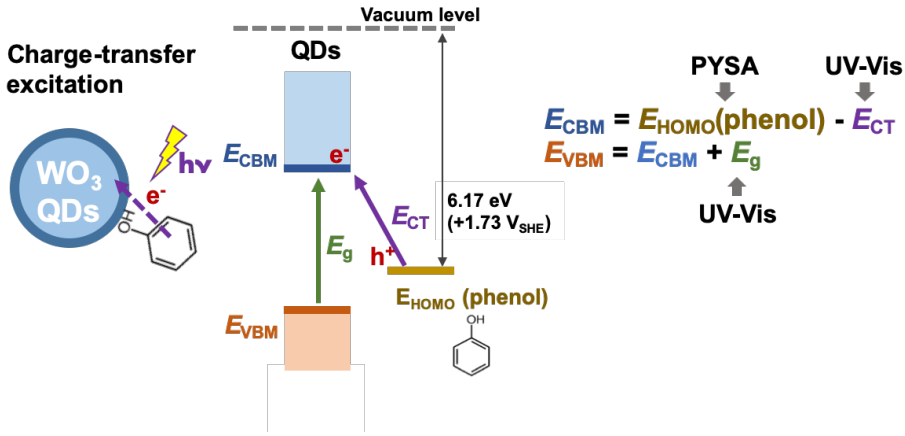

Fig. S6 A Schematic illustration of the band-edge energy determination of WO_3 QDs using a charge-transfer excitation.

Table S1 Charge-transfer excitation energy (E_{CT}), band-gap energy (E_g), energy level of the conduction band minima (E_{CBM} vs vacuum level) and valence band maxima (E_{VBM} vs vacuum level) of bulk WO_3, the as-prepared WO_3 QD, and the stabilized WO_3 QD.

	E_{CT} (eV)	E_g (eV)	E_{CBM} (eV)	E_{VBM} (eV)
Bulk WO_3	1.50	2.54	4.67 (+0.23 V_{SHE})	7.21 (+2.77 V_{SHE})
As-prepared WO_3 QD	1.94	3.10	4.23 (-0.21 V_{SHE})	7.33 (+2.89 V_{SHE})
Stabilized WO_3 QD	2.30	3.50	3.87 (-0.57 V_{SHE})	7.37 (+2.93 V_{SHE})

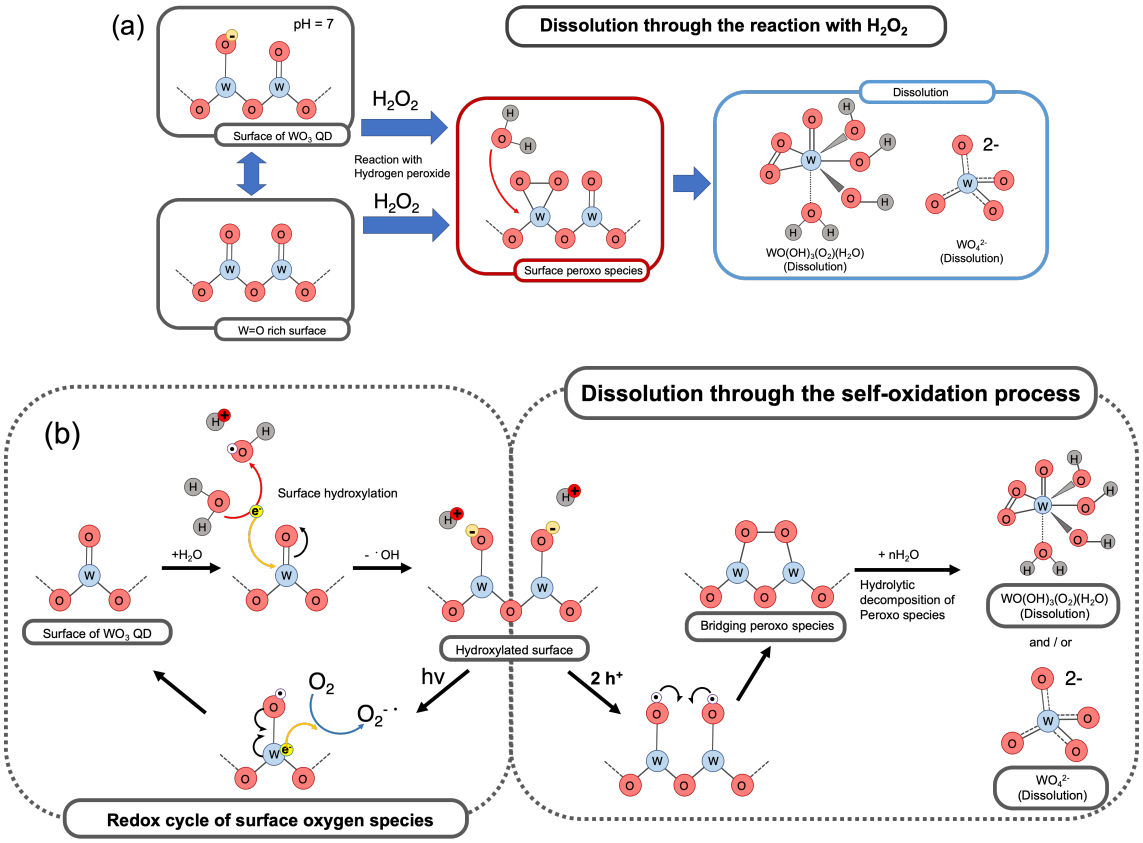

Fig. S7 Schematic illustration of dissolution mechanism for WO_3 QDs. (a) Dissolution through the reaction with H_2O_2. (b) Dissolution through the self-oxidation process by photo-generated holes.

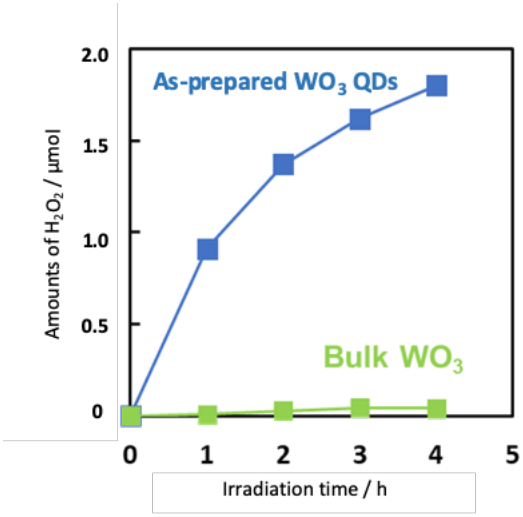

Fig. S8 Production of H_2O_2 with bulk WO_3 and as-prepared WO_3 QDs under UV illumination.

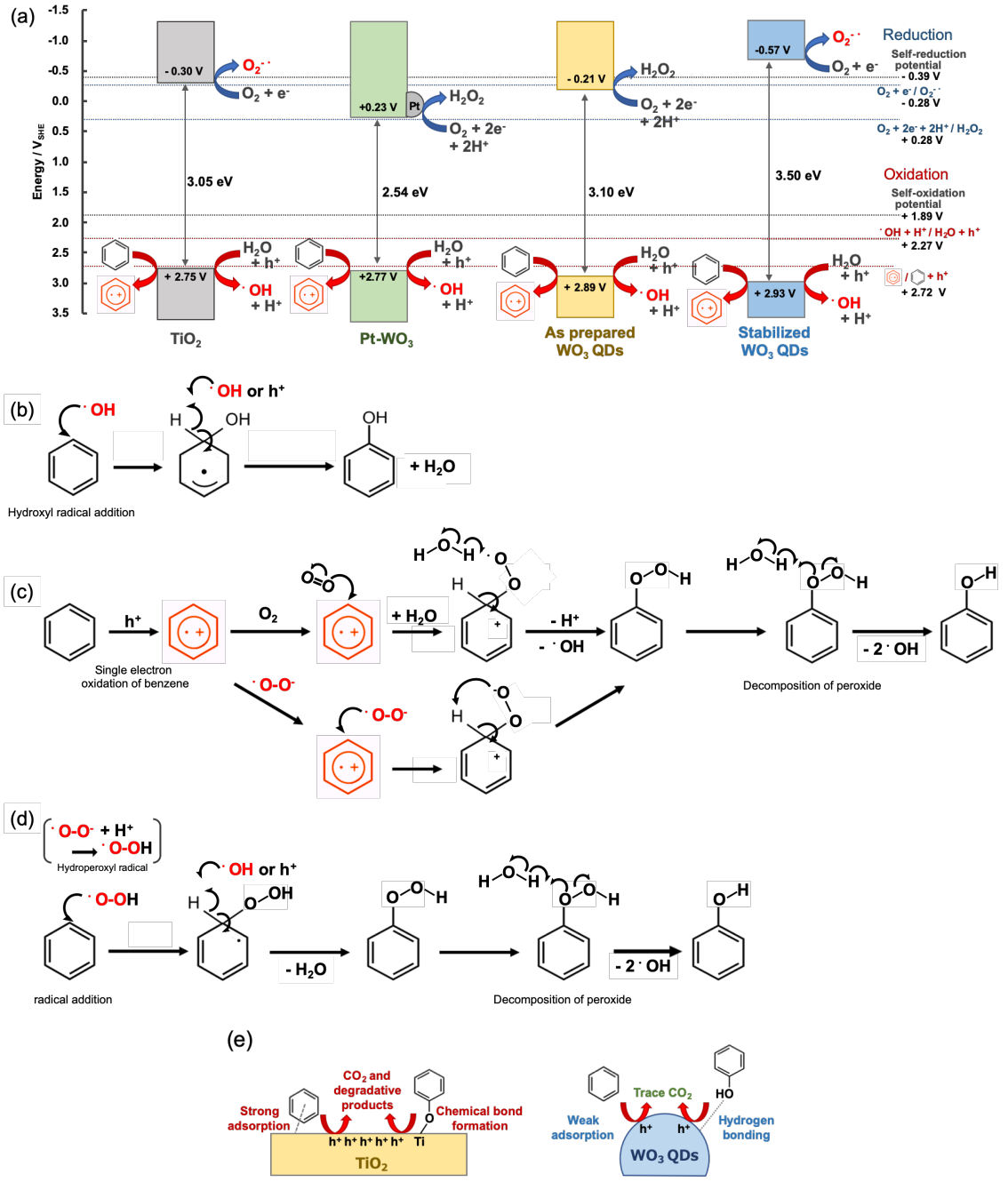

Fig. S9 Schematic illustrations of the photocatalytic reaction routes from benzene to phenol. (a) The energy diagrams and photo-produced active species for TiO_2, Pt-WO_3, as-prepared WO_3 QDs, and stabilized WO_3 QDs. (b-d) The reaction mechanisms of phenol production from benzene with different reaction routes. The key active species produced by the photocatalytic redox reactions were marked with red color. (b) promoted by hydroxyl radical (·OH), (c) promoted by benzene radical cation and superoxide radical, (d) promoted by superoxide radical ($O_2^{\cdot-}$). (e) The differences in the decomposition process between TiO_2 and WO_3 QDs.

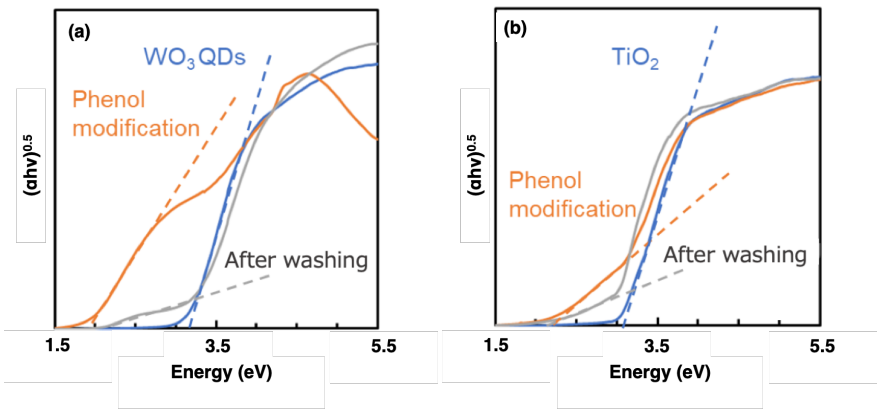

Fig. S10 Tauc plots before and after phenol modification (a) WO_3 QDs and (b) TiO_2.

The amount of phenol adsorbed on WO_3 QDs was greater than that on TiO_2 because of a higher specific surface area of the QDs. Phenol on WO_3 drastically decreased by washing with water, although a half of adsorbed phenol molecules remained on the TiO_2 surface.

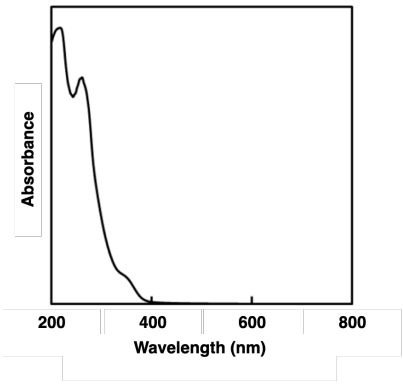

Fig. S11 A typical UV-vis spectrum of the resultant solution after photochemical dissolution for 8 h.

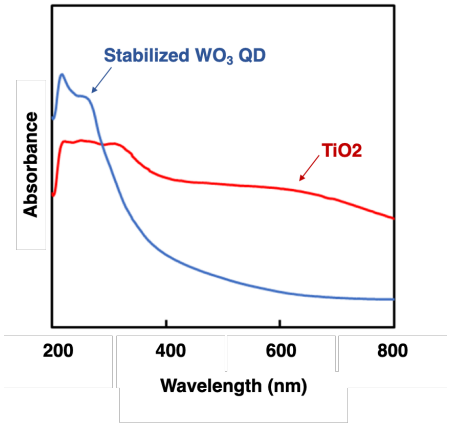

Fig. S12 UV-vis absorption spectra of stabilized WO_3 QDs and TiO_2 after the photochemical phenol formation under UV illumination. The presence of absorption in the visible region indicates that a large amount of photodegradates were adsorbed on TiO_2 after the illumination.

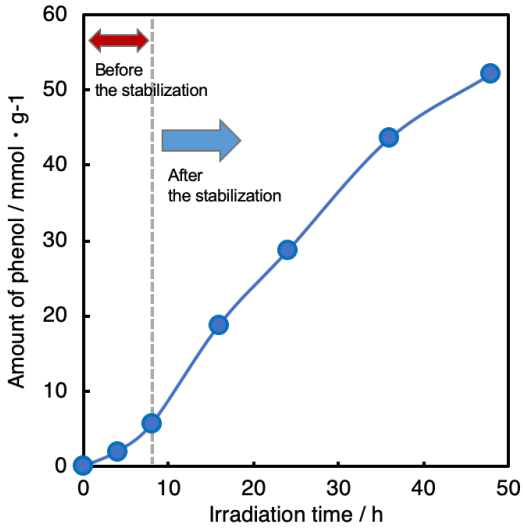

Fig. S13 The amounts of phenol produced with WO_3 QDs under UV illumination for before and after the stabilization. The data for the reaction time before the stabilization (< 8 h) were calculated by using average weight of the remaining WO_3 QDs in the periods (0-4 h: 8.39 mg, 4-8 h: 4.06 mg). Note that in the first 8h irradiation, the dissolution of the WO_3 QDs (the size reduction of the particles and the upshift of CBM) and the phenol production took place simultaneously. For the periods before the stabilization, the reaction efficiency was increased by the irradiation time because of the increase in the CBM level caused by size reduction of the WO_3 QDs. In contrast, the reaction efficiency was almost constant for the periods after the stabilization.

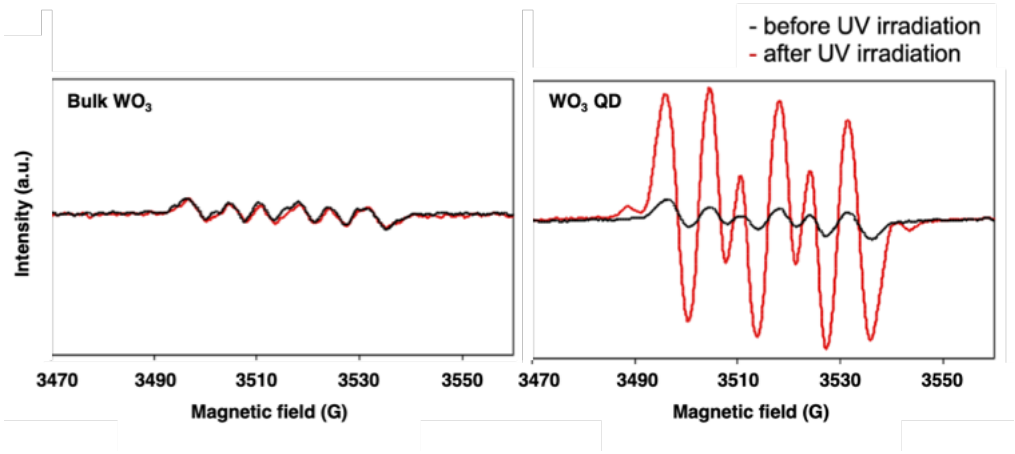

Fig. S14 Electron spin resonance spectra of a DMPO ethanolic solution before (black line) and after (red line) UV irradiation in bulk WO_3 and WO_3 QDs.[1]

$$O_2 + e^- \rightarrow \cdot O_2^-$$

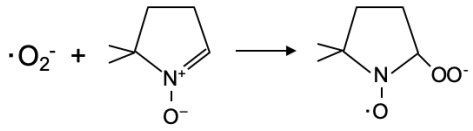

DMPO ·DMPO-OO-

ESR spin trapping experiment[1]

A 40 mM 5,5-dimethyl-1-pyrroline N-oxide (DMPO) ethanol solution was freshly prepared before usage. WO_3 QDs (E_g = 3.4 eV) or bulk WO3 was added to the DMPO solution and dispersed by weak ultra-sonication. The bulk WO_3 was prepared by calcinations of the H_2WO_4 at 873 K for 3 h. The particle concentration was set to 40 mg/mL and 4.0 mg/mL WO_3 QDs and bulk WO3, respectively, to keep the ideal weight of WO_3 constant. Each suspension was introduced in an ESR flat cell and placed horizontally during the UV irradiation to prevent sedimentation of the particles. The ESR spectra were measured before and after 90 min irradiation by 6 W UV-lamp (254 nm) as a light source.

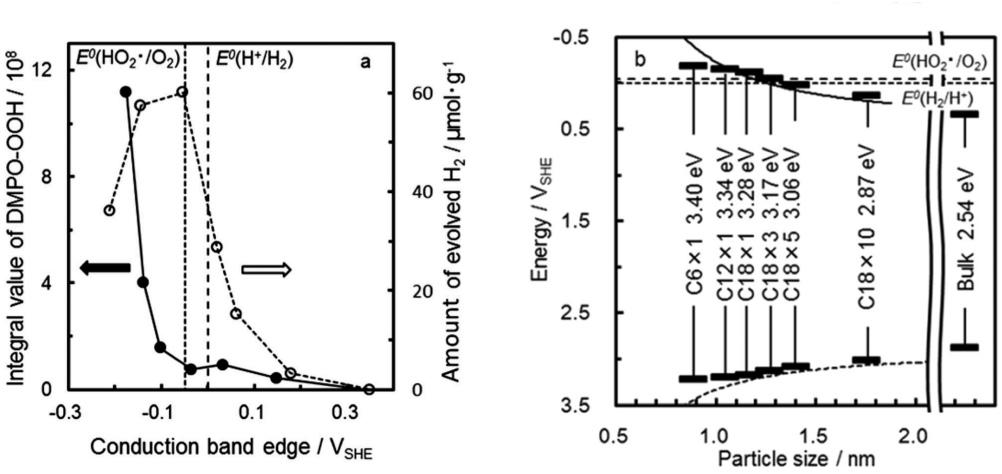

Fig. S15 (a) The relationship between the efficiency of photoreduction of proton (open circle) and molecular oxygen (closed circle) and the CBM potential of WO_3 QDs.[2] (b) The particle-size dependence of the CBM and VBM potentials. The experimental value (solid bar) and calculated value by the effective mass approximation theory (solid slope).[2] Reproduced from Refs. 1 and 2 with permission from the Royal Society of Chemistry.

The conversion of benzene, the yield of phenol based on the initial concentration of solubilized benzene in the aqueous reaction system. And the photocatalytic efficiency based on the unit time and weight of the catalysts.

The conversion of benzene after 40 h

(1 - ([benzene] – [CO_2] / 6 – [phenol]) / [benzene]) x 100 = 8.26 %

The conversion of benzene per unit time and weight of the catalyst

([benzene] – [CO_2] / 6 – [phenol]) / 40 h / 1.3 mg = 1.06 mmol/gh

The yield of phenol after 40 h

[phenol] / [benzene] x 100 = 8.25 %

The production efficiency of phenol per unit time and weight of the catalyst

[phenol] / 40 h / 1.3 mg = 1.06 mmol/gh

[CO_2]: The produced amount of CO_2 during the decomposition of phenol (~ 0.00025 mmol)

[phenol]: The produced amount of phenol after 40 h (0.05 mmol)

[benzene]: The amount of benzene solubilized in the system (0.67 mmol)

Table S2 Photocatalytic efficiency per unit time and weight of the catalysts.

Photocatalyst	Weight of Catalyst (mg)	Reaction time (h)	Produced amount of phenol (μmol)	Conversion rates of benzene (mmol/gh)	Selectivity (%)	Production rates of phenol (mmol/gh)
Stabilized WO_3 QD[(a)]	1.3	40.0	55.2	1.06	>99	1.06
Pt-WO_3[(a)]	10.0	48.0	30.0	0.06	>99	0.06
TiO_2-P25[(a)]	10.0	48.0	52.0	-[(c)]	-[(c)]	0.11
TiO_2-P[(b)]	10.0	4.0	3.2	0.39	20.8	0.08
Pt/TiO_2-P[(b)]	10.0	4.0	2.4	0.28	21.8	0.06
Pt/WO_3-K[(b)]	10.0	4.0	9.5	0.32	73.7	0.24

(a) This work. (b) The data calculated from ref 7. (c) The conversion and the selectivity could not be determined because benzene and phenol were mostly decomposed into surface degradates.

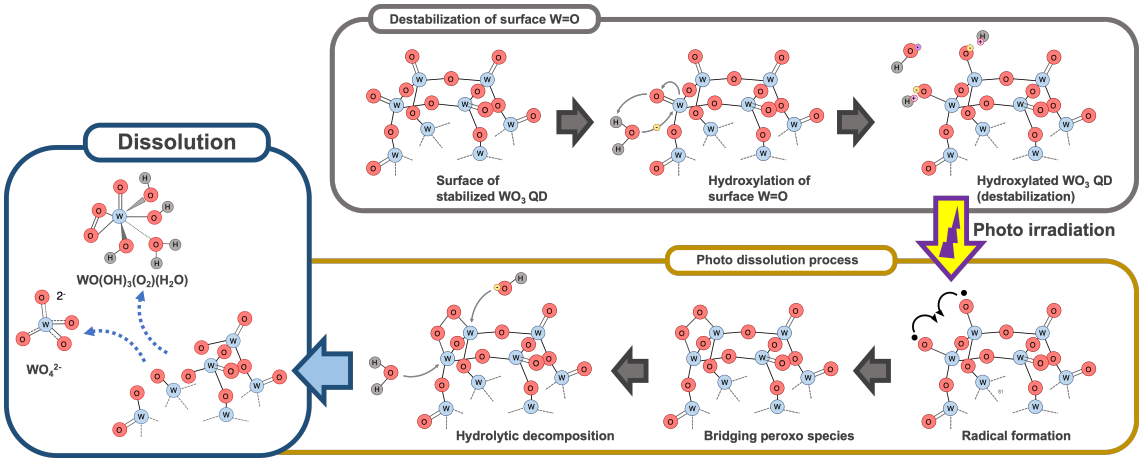

Fig. S16 Schematic illustration of a plausible mechanism for destabilization and re-dissolution of stabilized WO_3 QDs.

References

S1 H. Watanabe, K. Fujikata, Y. Oaki and H. Imai, *Chem. Commun.*, 2013, **49**, 8477–8479.

S2 T. Suzuki, H. Watanabe, Y. Oaki and H. Imai, *Chem. Commun.*, 2016, **52**, 6185–6188.

S3 O. Tomita, B. Ohtani and R. Abe, *Catal. Sci. Technol.*, 2014, **4**, 3850–3860.